JOURNAL OF SOLID STATE CHEMISTRY **133,** 379–385 (1997)
ARTICLE NO. SC977477

Crystal Structure Refinement and Stability of $LaFe_xNi_{1-x}O_3$ Solid Solutions

H. Falcón,* A. E. Goeta,† G. Punte,† and R. E. Carbonio*,[1]

** Instituto de Investigaciones en Fisicoquímica de Córdoba (INFIQC), Departamento de Fisicoquímica, Facultad de Ciencias Químicas, Universidad Nacional de Córdoba, Agencia Postal 4, Casilla de Correos 61, 5000 Córdoba, Argentina; and † PROFINO, Departamento de Física, Facultad de Ciencias Exactas, Universidad Nacional de La Plata, Casilla de Correos 67, 1900 La Plata, Argentina*

Received January 6, 1997; in revised form May 13, 1997; accepted May 21, 1997

The crystal structure refinement of $LaFe_xNi_{1-x}O_3$ ($0 \le x \le 1$) solid solutions was determined and analyzed by means of Rietveld refinement from X-ray powder diffraction data. The solid solutions with $0 \le x < 0.5$ are isostructural with $LaNiO_3$ and crystallize in the rhombohedral system, space group $R\bar{3}c$, while those with composition $0.5 < x \le 1$ are isoestructural with $LaFeO_3$ and crystallize in the orthorhombic system, space group *Pnma*. All of the solutions are single phase except that with the intermediate composition ($x = 0.5$), where both phases are observed. The cell volume increases with the iron content. This can be ascribed to the larger ionic radius of Fe^{3+} (HS) compared to Ni^{3+} (LS). $LaFe_{0.25}Ni_{0.75}O_3$ was found to be single phase when prepared at temperatures as high as 1000°C, indicating an increase in the stability of the perovskite phase at high temperatures when a relatively small amount of iron is substituted for Ni in $LaNiO_3$. © 1997 Academic Press

INTRODUCTION

Perovskite-type oxides with the general formula ABO_3, where A can be an alkali, alkaline earth, or a lanthanide metal and B may be a transition metal, play an important role in the preparation of catalysts serving for specific applications (1, 2). Their composition can be varied in a wide range by partial substitution of cations in positions A and B yielding compounds of the formula $(A_xA'_{1-x})(B_yB'_{1-y})O_3$.

Substitutional solid solutions are of main interest for catalytic purposes, since they allow the preparation of isostructural series with different physical properties and oxidation states of the B ion (3–5).

We have previously studied the catalytic properties of $LaFe_xNi_{1-x}O_3$ for peroxide decomposition and oxygen reduction. Very good catalytic activity was observed for intermediate compositions (6, 7). $LaFe_xNi_{1-x}O_3$ perovkites have been extensively studied using infrared spectroscopy (8), Mössbauer spectroscopy (8–11), magnetic measurements (7, 9–10) and electrical resistivity measurements (12, 13). However, no detailed structural studies have been undertaken thus far. A change from rhombohedral to orthorhombic symmetry has been reported for the $x = 0.5$ phase (10), but no refined parameters were presented. Although Asai *et al.* (9) reported that solid solutions were obtained only in the range ($0 \le x < 0.3$), a continuous range of solid solutions were found by other authors (8–10, 14).

One of the end members of the series, $LaNiO_3$, belongs to the rhombohedral system, space group $R\bar{3}c$ (No. 167). For the sake of convenience, a hexagonal description of the unit cell has been selected with parameters $a = 5.4573(3)$ and $c = 13.1601(6)$ Å (15). $LaNiO_3$ shows Pauli's paramagnetism and metallic properties. It is sensitive to partial oxygen pressures at high temperatures, since Ni(III) can be partially reduced to Ni(II) in air to produce oxygen vacancies; thus its composition may be better expressed as $LaNiO_{3-\delta}$ (16). On the other end of the series, $LaFeO_3$ belongs to the orthorhombic system, space group *Pnma* (No. 62) with parameters $a = 5.5647(1)$, $b = 7.8551(1)$, and $c = 5.5560(1)$ Å (17, 18); it is an antiferromagnetic insulator with a Neel temperature $T_N = 750$ K (19, 20).

We report here Rietveld refinement of X-ray powder diffraction data of $LaFe_xNi_{1-x}O_3$ solid solutions for $x = 0$; 0.10; 0.15; 0.25; 0.40; 0.50; 0.60; 0.75; 0.90; 1.00 synthesized at 900°C (except for $x = 0$ which was synthesized at 800°C) and of $LaFe_{0.25}Ni_{0.75}O_3$ prepared at different temperatures ($T_{sint} = 800$, 900, 1000, 1100°C).

EXPERIMENTAL

All of the compounds were prepared by the citrate amorphous precursor decomposition method (6, 21). The X-ray diffraction data of the powder samples were recorded using a Phillips PW-170 diffractometer with Cu$K\alpha$ radiation, between $20 \le 2\theta \le 120°$, with steps of 0.02° and counting time of 10 s per step.

[1] To whom correspondence should be addressed.

0022-4596/97 $25.00

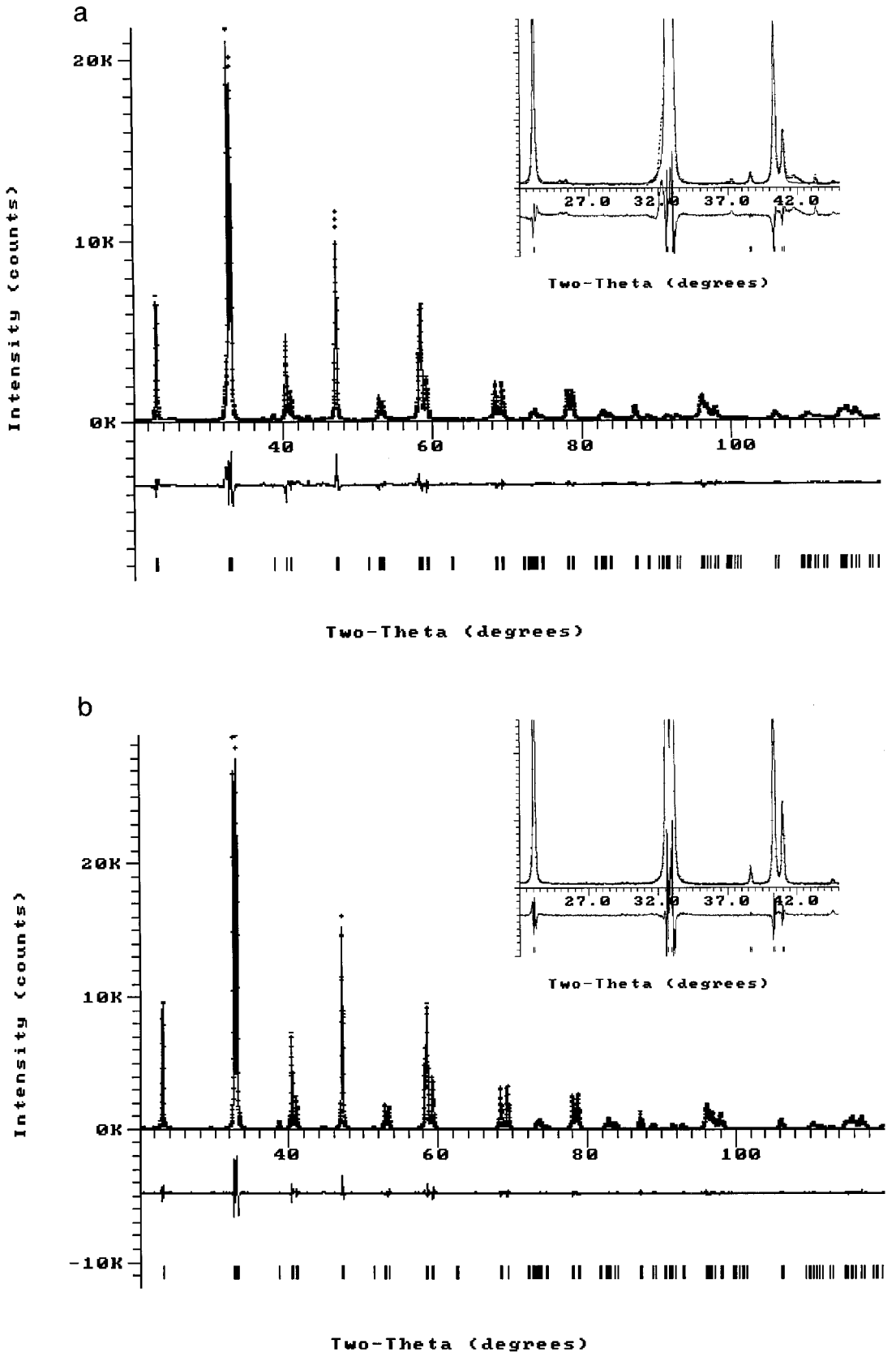

FIG. 1. (a) X-ray diffraction pattern of $LaFe_{0.25}Ni_{0.75}O_3$ ($T_{sint} = 1100°C$). (b) X-ray diffraction pattern of $LaFe_{0.25}Ni_{0.75}O_3$ ($T_{sint} = 1000°C$).

TABLE 1
Final Refinement Values of Cell Parameters and *R* Values for $LaFe_{0.25}Ni_{0.75}O_3$ Synthesized at Different Temperatures

$LaFe_{0.25}Ni_{0.75}O_3$	a/Å	c/Å	R_{exp}	R_{wp}	R_{Bragg}
$T_{sint} = 800°C$	5.4847(1)	13.2384(1)	4.86	10.05	3.74
$T_{sint} = 900°C$	5.4842(1)	13.2187(1)	5.03	9.37	3.19
$T_{sint} = 1000°C$	5.4864(1)	13.2084(1)	4.84	9.08	2.65
$T_{sint} = 1100°C$	5.4877(1)	13.2169(1)	5.02	14.65	6.46

The data were analyzed by means of the Rietveld method using the DBWS-9411 program (22). The initial atomic coordinates were taken from the literature (15, 18). The structure factors were calculated using the atomic scattering factors. The background was fitted with a polymonial function. The zero point, half-width, Pearson, and asymmetry parameters for the peak shape, scale factor, positional, and isotropic thermal parameters for all of the atoms and unit-cell parameters were refined.

RESULTS AND DISCUSSION

We have previously reported the X-ray diffraction results of $LaNiO_3$ synthesized at different temperatures (6). Only the burned amorphous citrate precursor was found at 500°C while at $600°C \leq T \leq 800°C$, a perovskite structure with a well-developed diffractogram was obtained. The number of reflections increased at $T \geq 900°C$ indicating that the decomposition of the perovskite phase starts in this temperature range. This is in agreement with the general reaction (23, 24)

$$(n+1)LaNiO_3 \rightarrow La_{n+1}Ni_nO_{3n+1} + NiO + 1/2O_2, \quad [1]$$

where $La_{n+1}Ni_nO_{3n+1}$ is a homologous series of layered Ruddlesden–Popper compounds (25–27). Because of this decomposition, in the present work $LaNiO_3$ was synthesized at 800°C.

Since $LaFe_{0.25}Ni_{0.75}O_3$ showed the highest catalytic activity for peroxide decomposition (6), we were interested in determining the temperature range in which the perovskite structure is stable for this composition.

For this purpose X-ray diffraction experiments were run for $LaFe_{0.25}Ni_{0.75}O_3$ synthesized at temperatures between 800 and 1100°C. The results of the refinements are shown in Table 1. It is clear from the obtained R values that when 25% of iron is introduced in the B site of $LaNiO_3$, temperatures of synthesis as high as 1000°C can be used without observing decomposition. This is in contrast to $LaNiO_3$, which decomposes at temperatures higher than 860°C (23–27). A slight decomposition, evidenced by the high R_{wp} value and by some impurity lines (shown in the inset of Fig. 1a) can be observed at 1100°C. A Rietveld refinement performed on the X-ray data of the samples obtained at 1000 and 1100°C are shown in Fig. 1. In the inset we show the region where the largest discrepancy between the calculated and experimental diagrams is observed. Therefore, it seems that the introduction of only 25% of Fe(III) in the position of Ni(III) considerably increases the stability of the perovskite phase at high temperatures. This increase in stability might be assigned to the higher stability of Fe(III) compared to Ni(III), which can be easily reduced.

For the $LaFe_xNi_{1-x}O_3$ series synthesized at 900°C (except for $LaNiO_3$ which was synthesized at 800°C) either rhombohedral or orthorhombic space groups were considered depending on the lines observed in the diffraction pattern. The rhombohedral distortion of the ideal perovskite octahedra is characterized by a splitting of the main reflections, whereas the orthorhomic distortion shows additional superstructural reflections with low intensity of the Bragg positions far from the characteristic reflections of the ideal perovskite (28). For all intermediate composition superstructural reflections, which might suggest long range order of Fe and Ni, were not observed. The Ni(III) and Fe(III) cations were assumed to be randomly distributed in the same crystallographic positions. Very small amounts of NiO were observed for some samples. This amount was

TABLE 2
Final Refinement Values of Cell Parameters, Normalized Cell Volume (V/Z), Density and *R* Values for the $LaFe_xNi_{1-x}O_3$ Series Prepared at 900°C (Except for $LaNiO_3$ Which Was Prepared at 800°C)

Compound	a/Å	b/Å	c/Å	(V/Z)/Å^3	ρ/(g cm^{-3})	Space group	R_{wp}	R_{Bragg}	R_{exp}
$LaNiO_3$	5.4573(3)	5.4573(3)	13.1601(6)	56.57	7.214	$R\bar{3}c$	14.74	7.76	6.66
$LaFe_{0.10}Ni_{0.90}O_3$	5.4670(1)	5.4679(1)	13.1694(1)	56.81	7.178	$R\bar{3}c$	9.77	3.57	5.67
$LaFe_{0.15}Ni_{0.85}O_3$	5.4714(1)	5.4714(1)	13.1833(1)	56.96	7.149	$R\bar{3}c$	9.59	3.11	5.66
$LaFe_{0.25}Ni_{0.75}O_3$	5.4850(1)	5.4850(1)	13.2198(1)	57.40	7.087	$R\bar{3}c$	9.37	3.19	5.03
$LaFe_{0.40}Ni_{0.60}O_3$	5.5047(1)	5.5047(1)	13.2642(1)	58.01	6.999	$R\bar{3}c$	10.43	2.85	5.17
$LaFe_{0.60}Ni_{0.40}O_3$	5.4907(3)	7.7830(3)	5.5278(3)	59.06	6.860	*Pnma*	9.96	2.98	7.31
$LaFe_{0.75}Ni_{0.25}O_3$	5.5203(1)	7.8142(2)	5.5390(1)	59.73	6.769	*Pnma*	7.65	2.68	5.29
$LaFe_{0.90}Ni_{0.10}O_3$	5.5485(1)	7.8401(1)	5.5495(1)	60.35	6.689	*Pnma*	10.13	3.35	6.38
$LaFeO_3$	5.5647(1)	7.8551(1)	5.5560(1)	60.71	6.504	*Pnma*	10.39	2.63	7.79

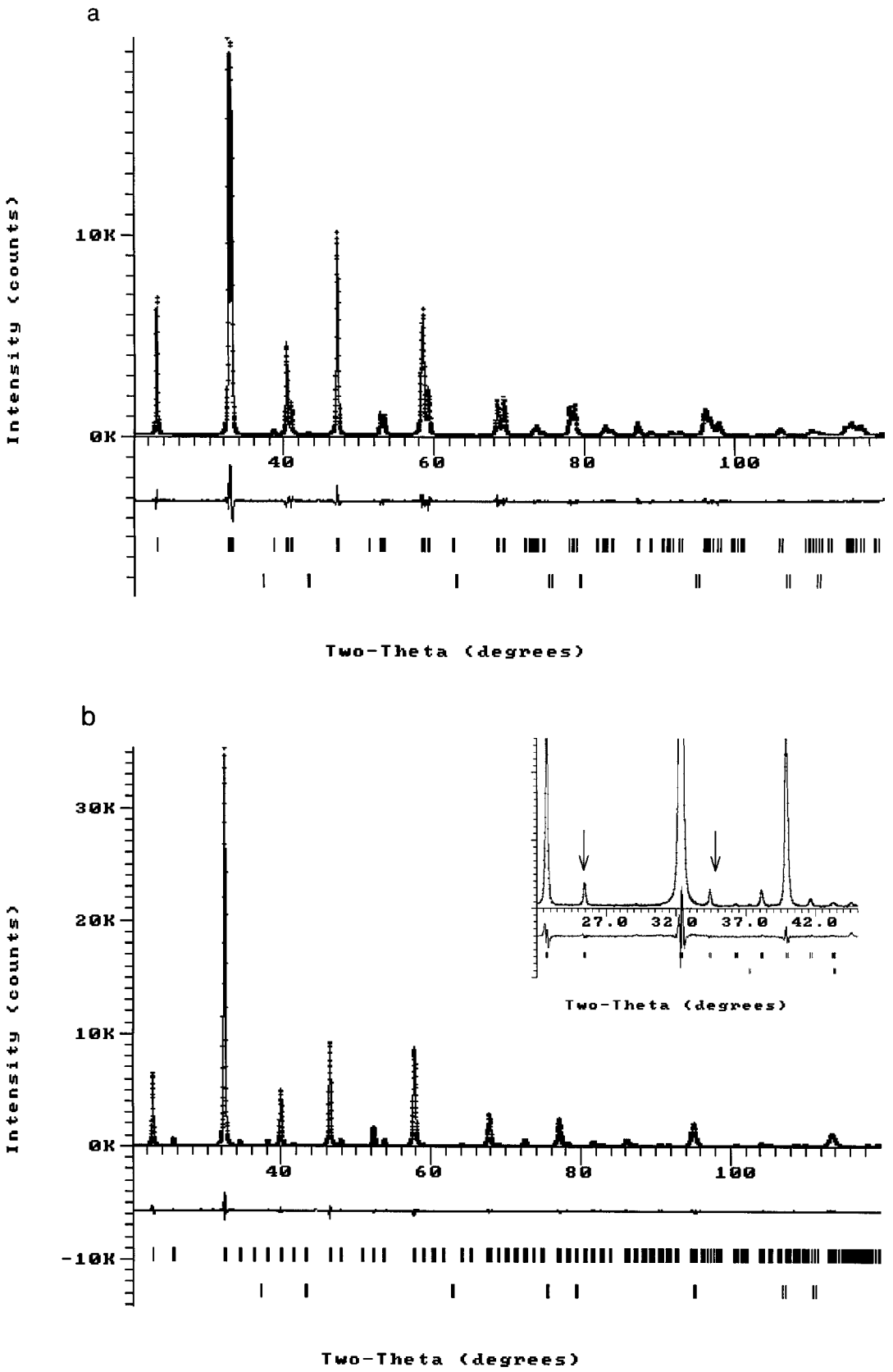

FIG. 2. (a) X-ray diffraction pattern of $LaFe_{0.25}Ni_{0.75}O_3$ ($T_{sint} = 900°C$). (b) X-ray diffraction pattern of $LaFe_{0.75}Ni_{0.25}O_3$ ($T_{sint} = 900°C$).

always lower than 0.4%. Only for one intermediate composition, $LaFe_{0.50}Ni_{0.50}O_3$, both the rhombohedral and orthorhombic phases were simultaneously identified. For this reason a model including both crystallographic phases was refined.

Figure 2 shows the observed and calculated profiles and their differences after the refinement for two representative compositions (one for each crystal system). In the inset, the region where the superstructure reflections with low intensity (marked with arrows) appear for the orthorhombic system is shown. The discrepancy factors, R, and final refinement parameters are listed in Table 2. The dependence of refined cell parameters with composition for both phases is shown in Figs. 3 and 4.

In order to compare volume changes for both phases, we defined the normalized volume (V/Z), where Z is the number of formulas per unit cell. We show its dependence with composition in Fig. 5. There is an increase of V/Z as the iron content increases. This effect can be easily understood considering the ionic radii of Ni(III) (low spin) and Fe(III) (high spin) which are 0.56 and 0.645 Å, respectively (29). Two straight lines were obtained, one for each type of phase.

Table 3 lists the refined oxygen positions and thermal isotropic factors for La, (Ni, Fe) and O for the rhombohedral phases (space group $R\bar{3}c$). Although the variation of $x_{(O)}$ is not strictly regular, it tends to increase as the iron content increases. Taking into account that in an ideal perovskite, without distortion, this parameter is 0.50 (30), the progressive deviation from this value accounts for a progressive increase of the tilting of the octahedras $(Ni, Fe)O_6$ and therefore of the distortion of perovskite as x increases. An extremely large value of $B_{(O)}$ was obtained for $LaNiO_3$. A possible explanation could be that because $LaNiO_3$ contains a relatively large amount of oxygen vacancies, during the refinement this is artificially accounted by increasing $B_{(O)}$. The refinement of the occupation factor of O cannot be performed with powder X-ray data because of the very low value of the O scattering factor.

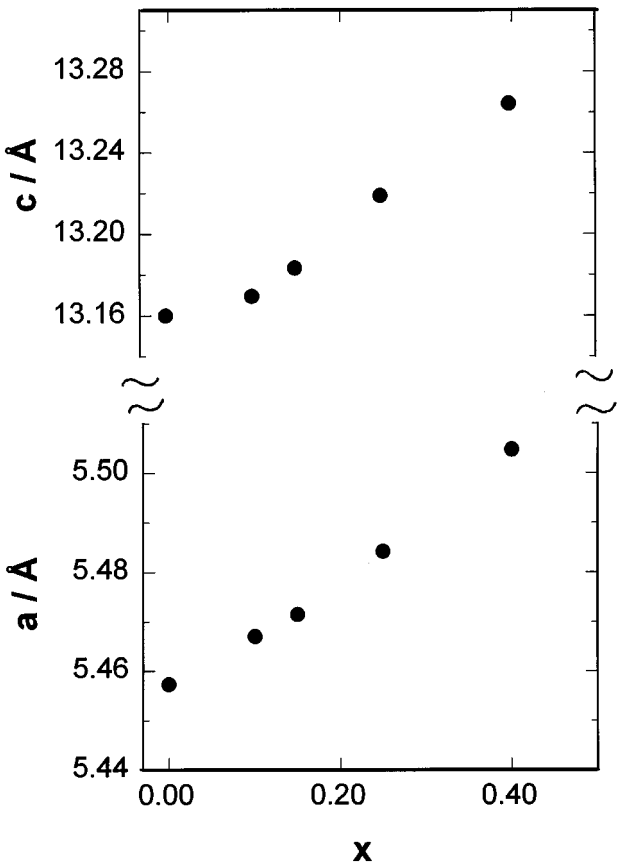

FIG. 4. Dependence of the cell parameters with composition for $LaFe_xNi_{1-x}O_3$. $T_{sint} = 900°C$ $(0 \leq x < 0.5)$.

Table 4 includes atomic positions and temperature factors for the orthorhombic phases (space group *Pnma*). In

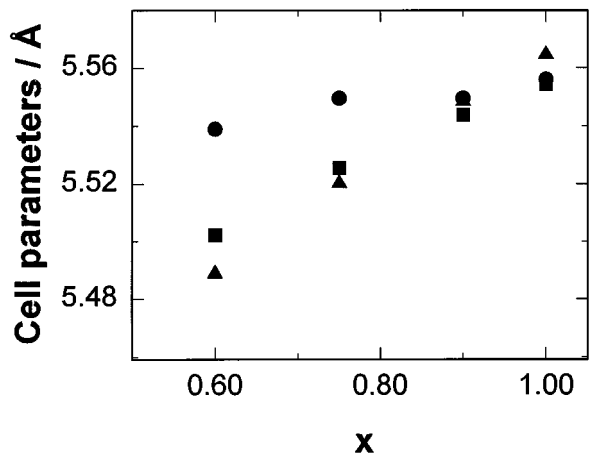

FIG. 3. Dependence of cell parameters a, ▲; b, $\sqrt{2}$, ●; c, ■ with composition for $LaFe_xNi_{1-x}O_3$. $T_{sint} = 900°C$ $(0.5 < x \leq 1.0)$.

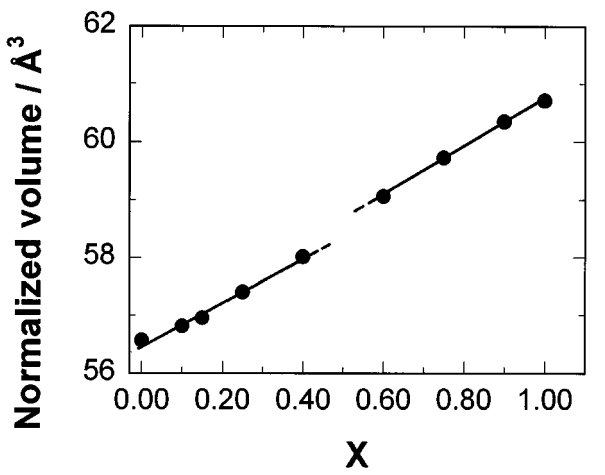

FIG. 5. Dependence of the unit-cell normalized volume (V/Z) with composition for $LaFe_xNi_{1-x}O_3$. $T_{sint} = 900°C$.

TABLE 3
Atomic Positions and Temperature Factors for $LaFe_xNi_{1-x}O_3$ with $0 \leq x < 0.5$ (Space Group $R\bar{3}c$)

Compound	$x_{(O)}$	$B_{(La)}/Å^2$	$B_{(Ni,Fe)}/Å^2$	$B_{(O)}/Å^2$
$LaNiO_3$	0.5329(1)	0.516(1)	0.357(1)	2.88(1)
$LaFe_{0.10}Ni_{0.90}O_3$	0.5448(7)	0.59(2)	0.49(2)	1.55(9)
$LaFe_{0.15}Ni_{0.85}O_3$	0.5480(7)	0.61(2)	1.01(9)	1.25(9)
$LaFe_{0.25}Ni_{0.75}O_3$	0.5481(1)	0.66(2)	0.46(2)	1.42(9)
$LaFe_{0.40}Ni_{0.60}O_3$	0.5514(7)	0.69(2)	0.46(3)	1.07(1)

Note. La occupies the sites (16*a*) (0, 0, 1/4); (Ni, Fe) are at (6*b*) (0, 0, 0) and oxygens are at (18*e*) (x, 0, 1/4).

TABLE 5
Tolerance Factors (t) for $LaFe_xNi_{1-x}O_3$

Compound	(Fe, Ni)–O/Å	t	Symmetry of phases
$LaNiO_3$	1.960	0.996	R
$LaFe_{0.10}Ni_{0.90}O_3$	1.969	0.991	R
$LaFe_{0.15}Ni_{0.85}O_3$	1.973	0.989	R
$LaFe_{0.25}Ni_{0.75}O_3$	1.981	0.985	R
$LaFe_{0.40}Ni_{0.60}O_3$	1.994	0.979	R
$LaFe_{0.50}Ni_{0.50}O_3$	2.003	0.974	R–O
$LaFe_{0.60}Ni_{0.40}O_3$	2.011	0.970	O
$LaFe_{0.75}Ni_{0.25}O_3$	2.024	0.964	O
$LaFe_{0.90}Ni_{0.10}O_3$	2.037	0.958	O
$LaFeO_3$	2.045	0.954	O

these phases the parameter $y_{(O2)}$ as well as $z_{(O2)}$ are sensitive to the effect of the tilting of the octahedra (30). Data corresponding to the composition $LaFe_{0.50}Ni_{0.50}O_3$, which is a mixture of both phases, are omitted. A gradual increase of $y_{(O2)}$ occurs as the composition approaches $LaNiO_3$ which has the greatest structural distortion in this series.

The two different symmetries observed in the different compositional ranges of this series can be explained in terms of the simple ionic model described by Goldschmidt (2). According to this model, a tolerance factor (t) can be defined as $t = d_{A-O}/\sqrt{2}d_{B-O}$. For the ideal cubic perovskite, this value should be around 1. For t values slightly less than 1, the BO_6 octahedra are rotated about the (111) axis and a rhombohedral distortion is observed, such as in $LaNiO_3$. For smaller t, the octahedra tilt about (110) and (001) axis and an orthorhombic distortion is found as in $LaFeO_3$. Table 5 lists the values of t calculated from the distances A–O and B–O obtained by the addition of the ionic radii. For these calculations we have taken the 12-coordinated effective ionic radius of La^{3+} (1.36 Å); the 6-coordinated radii for Ni^{3+} (LS) (0.56 Å) and Fe^{3+} (HS) (0.645 Å) and 1.40 Å for O^{2-} (29). For the intermediate compositions, the value (Fe, Ni)–O was obtained using the weighted average of the radii of Ni^{3+} and Fe^{3+}. A rhombohedral symmetry was observed experimentally for values of the tolerance factor between 0.996 and 0.979. For 0.974 a mixture of both phases was observed. For $t \leq 0.970$, the orthorhombic phase is clearly more stable. A similar behavior was reported by Lacorre *et al.* for $REMO_3$ compounds (where RE = rare earth and M = Cr, Al, Co, Cu, or Ni) (28).

CONCLUSIONS

$LaFe_{0.25}Ni_{0.75}O_3$ can be obtained as a single-phase material at temperatures as high as 1000°C. A slight decomposition is observed for this phase at 1100°C, which is evidenced by the high R_{wp} value obtained in the Rietveld refinement and by some impurity lines. Thus, the introduction of a small amount of Fe(III) in the positions of Ni(III) increases the stability of the perovskite phase at high temperatures.

For the $LaFe_xNi_{1-x}O_3$ series, the Rietveld refinement results indicated that all of the samples are monophasic except the one with composition $LaFe_{0.50}Ni_{0.50}O_3$. Those with $0 \leq x < 0.5$ show the $LaNiO_3$ structure, (rhombohedral system space group $R\bar{3}c$) while samples with $0.5 < x \leq 1$ show the $LaFeO_3$ structure (orthorhombic system, space group *Pnma*). For the sample with composition $LaFe_{0.50}Ni_{0.50}O_3$, both the rhombohedral and orthorhombic phases were found.

Cell parameters increase progressively with increasing Fe content and the normalized cell volume (V/Z) increases linearly with x due to the larger radius of Fe(III) (HS) compared to Ni(III) (LS).

TABLE 4
Atomic Positions and Temperature Factors for $LaFe_xNi_{1-x}O_3$ with $0.50 < x \leq 1$ (Space Group *Pnma*)

Compound	$x_{(O1)}$	$z_{(O1)}$	$x_{(O2)}$	$y_{(O2)}$	$z_{(O2)}$	$x_{(La)}$	$z_{(La)}$	$B_{(Ni-Fe)}/Å^2$	$B_{(O1)}/Å^2$	$B_{(O2)}/Å^2$	$B_{(La)}/Å^2$
$LaFe_{0.60}Ni_{0.40}O_3$	0.496(3)	0.071(2)	0.0276(4)	0.033(3)	−0.272(4)	0.0190(3)	−0.0032(4)	0.32(9)	0.78(3)	1.00(2)	0.67(4)
$LaFe_{0.75}Ni_{0.25}O_3$	0.4923(9)	0.073(2)	0.283(2)	0.030(3)	−0.279(2)	0.0283(1)	−0.0051(3)	0.54(2)	0.34(1)	2.23(3)	0.71(1)
$LaFe_{0.90}Ni_{0.10}O_3$	0.491(1)	0.067(3)	0.279(1)	0.035(1)	−0.285(1)	0.0272(1)	−0.0061(2)	0.23(2)	0.55(1)	1.76(1)	0.63(2)
$LaFeO_3$	0.489(1)	0.069(2)	0.281(1)	0.039(1)	−0.28(1)	0.0291(1)	−0.0061(2)	0.45(2)	0.64(3)	2.24(3)	0.68(1)

Note. La occupies the sites (4*c*) (x, 1/4, z); (Ni, Fe) are at (4*b*) (0, 0, 1/2); oxygens (O1) are at (4*c*) (x, 1/2, z) and (O2) at (8*d*) (x, y, z).

ACKNOWLEDGMENTS

R.E.C. thanks Consejo de Investigaciones Científicas y Tecnológicas de la Provincia de Córdoba (CONICOR), Secretaría de Ciencia y Tecnología of the Universidad Nacional de Córdoba, and Fundación Antorchas for research grants. G.P. thanks CONICET research grants. G.P. and R.E.C. are members of the "Carrera del Investigador," CONICET. We thank Dr. J. A. Alonso and R. Viña for helpful discussions. Data were obtained with a LANADI (CONICET–UNLP) diffractometer.

REFERENCES

1. L. G. Tejuca, *J. Less-Common Met*. **146,** 251 (1989).
2. J. G. Tejuca, J. L. G. Fierro, and J. M. D. Tascón, *Adv. Catal.* **36,** 237 (1989).
3. R. J. H. Voorhoeve, "Advanced Materials in Catalysis" (J. J. Burton and R. L. Garten, Eds.), p. 129. Academic Press, New York, 1977.
4. W. F. Libby, *Science* **171,** 499 (1971).
5. S. C. Sorteson, J. A. Wronbierwics, L. B. Sis, and G. P. Wirtz, *Bull. Am. Ceram. Soc*. **53,** 446 (1974).
6. H. Falcón and R. E. Carbonio, *J. Electroanal. Chem.* **339,** 69 (1992).
7. R. E. Carbonio, C. Fierro, D. Tryk, D. Scherson, and E. Yeager, *J. Power Sources* **22,** 387 (1988).
8. P. Ganguly and N. Y. Vasanthacharya, *J. Solid State Chem.* **61,** 164 (1986).
9. K. Asai and H. Sekizawa, *J. Phys. Soc. Jpn.* **49,** 90 (1980).
10. N. Y. Vasanthacharya, P. Ganguly, and C. N. R. Rao, *J. Solid State Chem.* **53,** 140 (1984).
11. A. E. Goeta, G. F. Goya, R. C. Mercader, G. Punte, H. Falcón, and R. Carbonio, *Hyperfine Interactions* **90,** 371 (1994).
12. P. Ganguly, N. Y. Vasanthacharya, C. N. R. Rao, and P. P. Edwards, *J. Solid State Chem.* **54,** 400 (1984).
13. A. Chainani, D. D. Sarma, I. Das, and E. V. Sampathkumaran, *J. Phys. Condens. Matter B*, 637 (1996).
14. N. Y. Vasanthacharya, K. K. Singh, and P. Ganguly, *Rev. Chim. Miner.* **18,** 333 (1981).
15. J. L. García Muñoz, J. Rodríguez Carvajal, P. Lacorre, and J. B. Torrance, *Phys. Rev. B* **46,** 4414 (1992).
16. J. A. M. Van Roosmalen and E. H. P. Cordfunke, *J. Solid State Chem.* **93,** 212 (1991).
17. S. Geller and E. A. Wood, *Acta Crystallogr.* **9,** 563 (1956).
18. H. L. Yakel, *Acta Crystallogr.* **8,** 394 (1955).
19. G. R. Hearne, M. P. Pasternak, R. D. Taylor, and P. Lacorre, *Phys. Rev. B* **51,** 11495 (1995).
20. D. Treves, *J. Appl. Phys.* **36,** 1033 (1965).
21. J. M. D. Tascón, S. Mendioroz, and L. González Tejuca, *Z. Phys. Chem.* **124,** 109 (1981).
22. R. A. Young, A. Sakthivel, T. S. Moss, and C. O. Paiva-Santos, *J. Appl. Crystallogr.* **28,** 366 (1995).
23. P. Odier, Y. Nigara, J. Coutures, and M. Sayer, *J. Solid State Chem.* **56,** 32 (1985).
24. J. Takahashi, T. Toyoda, T. Ito, and M. Takatsu, *J. Mater. Sci.* **25,** 1557 (1990).
25. C. Brisi, M. Vallino, and F. Abbattista, *J. Less-Common Met.* **79,** 215 (1981).
26. J. Drennan, C. P. Tavares, and B. C. H. Steele, *Mater. Res. Bull.* **17,** 621 (1982).
27. R. A. M. Ram, L. Ganapathi, P. Ganguly, and C. N. R. Rao, *J. Solid State Chem.* **63,** 139 (1986).
28. P. Lacorre, J. B. Torrance, J. Pannetier, A. I. Nazzal, P. W. Wang, and T. C. Huang, *J. Solid State Chem.* **91,** 225 (1991).
29. R. D. Shannon, *Acta Crystallogr. A* **32,** 751 (1977).
30. M. O'Keeffe and B. G. Hyde, *Acta Crystallogr. B* **33,** 3802 (1977).